

PRELIMINARY RESULTS ON A SAMPLE OF BE STARS OBSERVED WITH THE VEGA/CHARA INTERFEROMETER

Delaa, O.¹, Stee, P.¹, Zorec, J.² and Mourard, D.¹

Abstract.

It is well known that the Be phenomenon, i.e. presence of Balmer lines emission and infrared excess in the spectrum of Be stars, takes its origin in a rotating disk-like circumstellar environment. On the other hand, the origin, kinematics and geometry of those circumstellar environments are still hardly debated. In this contribution, we present the first results from the VEGA/CHARA interferometer observations of the classical Be star ψ Per. We have extracted the visibilities and differential phases from these interferometric data, mainly around the Balmer H_α and H_β emission lines, and tried to determine the geometry and kinematics of the concerned emitting regions.

1 Introduction

Classical Be stars are Main Sequence B-type stars with high rotational velocities, which are surrounded by a rotating flattened circumstellar environment, which produces the emission lines in spectrum of these objects. This circumstellar environment is also responsible for the measured infrared excess, due mainly to the free-free and free-bound transitions (Gehrz et al. 1974). These two most outstanding characteristics define what has been called the "Be phenomenon". The geometry and structure of these envelopes were intensively studied since Struve's scenario proposed in 1931, where the rapid rotation is responsible for a lens-shaped stellar photosphere and an equatorial ejection of matter that leads to the formation of a nebulous ring. There is now clear evidence for the geometry of these circumstellar envelopes being mostly flattened and axisymmetric (Dougherty & Taylor 1992; Hanuschik 1996; Quirrenbach 1997; Stee 2003). From the study of accretion disks it follows that disks in hydrodynamical equilibrium and in Keplerian rotation are very thin, since their vertical scale height is governed by the gas pressure only. For a disk to be thicker, either additional mechanisms have to be assumed, or the disk might not be in equilibrium (Bjorkman & Carciofi 2004). Be stars have "excretion" disks rather than "accretion" ones. The hydrostatic equilibrium might not only be determined by the gas pressure but also by magnetic fields (Arias et al. 2006, Zorec et al. 2007), so that their vertical scale height can increase. Another important property of "classical" Be disks is that their equatorial region must be characterized by a very low radial expansion velocity (Poeckert & Marlborough 1978; Waters et al. 1986, 1987, 1992). In a recent paper, Meilland et al. (2007) have confirmed that the equatorial disk around the Be star α Aps is in Keplerian rotation with a disk radial velocity of only few kms^{-1} . In addition to this rotating equatorial disk-like region, Be stars seem to have a much more rarefied region above and below the equatorial plan where the velocities may reach up to 1000 km/s, often called "polar winds". Evidence for such high velocity regions are found in the strong asymmetry of far-UV lines, which are formed in these regions (e. g. Marlborough 1987), and from the recent interferometric observations that put forward evidence for a polar wind along the rotational axis of Achernar (Kervella & Domiciano de Souza 2006).

Differential spectro-interferometry is a powerful tool to study the kinematics within the circumstellar environments. The shape of the differential phase of fringes across the $\text{Br}\gamma$ line profile is related to the photocenter

¹ Lab. H. Fizeau, CNRS UMR 6525, Univ. de Nice-Sophia Antipolis, Observatoire de la Cote d'Azur, Avenue Nicolas Copernic, 06130 Grasse, France. email: Omar.delaa@obs-azur.fr

² Institut d'Astrophysique de Paris, UMR 7095 du CNRS, Universite Pierre & Marie Curie, 98bis bd. Arago, 75014 Paris, France

displacement as a function of the wavelength and is very sensitive to the β exponent of the rotation power law used in the modeling of disks (Stee 1996). As already mentioned, by using a Keplerian rotation within the disk, Meilland et al. (2007) were able to obtain a very good agreement between the VLTI/AMBER data and the theoretically predicted visibilities and phases of the Br γ emission line as a function of wavelength, for four VLTI baselines.

Nevertheless, many questions regarding the origin of the Be phenomenon remain still unsolved and are source of intense debated. For instance, why some hot stars are able to form disks, but not others ? Why some disks appear and disappear quasi-cyclically ? What are the final geometry and kinematics of Be stars disks ? What is the incidence of these disks on the underlying star evolution ? Is the Be phenomenon due to binarity ?

The following paper deals with the study of the geometry and kinematics of the circumstellar disk around the Be star Ψ Per. It is structured as follows: In section 2, the VEGA/CHARA instrument and the observations of the classical Be stars Ψ Per are presented. In section 3, we summarize our main results. Some prospectives regarding the study of this star are drawn in section 4.

2 Observations

2.1 The VEGA/CHARA instrument

The Visible spEctroGraph and polArimeter (VEGA) instrument (Mourard et al. 2009) operates in the visible domain and combines a spectrograph with a polarimeter. The spectrograph is designed to sample data in the visible wavelengths from 0.45 to 0.85 μm . Two photon counting detectors in the blue and red spectral domains can record the dispersed fringes. The main characteristics of this spectrograph are summarized in Table 1.

Grating	R	$\delta\lambda(\text{blue})$	$\delta\lambda(\text{Red})$	$\lambda_R - \lambda_B$
R1: 1800 gr/mm	30000	5 nm	8 nm	25 nm
R2: 300 gr/mm	5000	30 nm	45 nm	170 nm
R3: 100 gr/mm	1700	100 nm	150 nm	not possible

Table 1. Spectral resolutions (Rx) and bandwidths ($\delta\lambda$) of the VEGA spectrograph, and the spectral separation between the two detectors.

Simultaneous observations with the two detectors are possible only in the high and medium spectral resolution modes. Thus, it is possible to record simultaneously data in the medium resolution mode around H α with the red detector and around H β with the blue detector. Nevertheless, the observations with the blue detector require good seeing conditions, which is the main reason that our results obtained with the blue detector are not as good as those with the red one. The medium (6000) and high (30000) spectral resolutions are well suited for studies of disk kinematics. They provide velocity resolutions of 60 and 10 kms^{-1} , respectively. The low (1700) and medium resolution powers are useful for absolute visibility measurements and for the study of binaries or multiple systems.

The polarimeter has a Wollaston prism to separate two orthogonal polarization states, and a movable quarter wave plate. A fixed quarter wave plate is placed after the Wollaston prism to transform the two linearly polarized output beams into two circularly polarized beams. This is done to avoid unbalanced transmissions by the grating. After being spectrally dispersed, the two beams carry each both the interference pattern and the polarization information. These are focused on the photon-counting detectors, which produce two (x, λ) images, one per polarization state, referred as "High" and "Low" polarizations with respect to their position on the detector. As previously detailed by Rousselet-Perraut et al. (2006), this polarimeter can measure three (I, Q, and V) over four Stokes parameters.

2.2 VEGA/CHARA observations

ψ Per was observed with VEGA using the CHARA array facilities located at the Mount Wilson Observatory (LA, California, USA). The Observations were carried out on 7, 8 and 9 October 2008. ψ Per was observed with the Red and Blue detectors, centered around 656 nm and 486 nm, respectively. We used the medium ($R = 5000$) spectral resolution, but no polarimetric mode observation was carried out for this star. For each observation, two over six 1 meter telescopes available within the CHARA array were used. Thus, no closure phase (which requires at least 3 telescopes) was available. Details on the observing run can be found in Table 2.

Object	date	Telescopes	baseline (m)	Orientation (deg)
ψ Per	07/10/2008 11h33	S1S2	32.35	-20.92
	08/10/2008 06h52	S1S2	32,54	18,38

Table 2. Observing logs

3 Results

The extensions of the emitting regions in the $H\alpha$ and $H\beta$ lines are determined from the modulus of the visibility. Figure 1 presents the evolution of the visibility modulus as a function of wavelength:

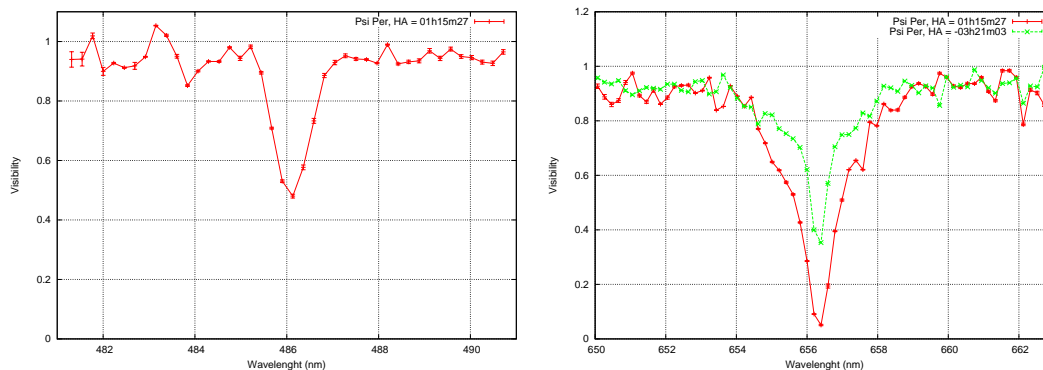


Fig. 1. Differential visibility across the $H\beta$ (left) and $H\alpha$ (right) lines for ψ Per, at HA indicated on the figure, for the S1S2.

The visibilities in the continuum nearby $H\alpha$ and $H\beta$ are close to one, which implies that the observed object is a point-like source in these two spectral domains, i.e. remains unresolved. Within the $H\alpha$ and $H\beta$ lines, we have a strong decrease of the visibility (stronger in $H\alpha$ than in the $H\beta$ line), which clearly indicates that the object extension in these two emission lines is larger than in the nearby continuum. The corresponding emitting regions can reach $10 R_{\star}$ (Tycner et al. 2008; Grundstrom & Gies 2006).

In Fig. 1 we can see that the $H\alpha$ visibilities (red and green) are different, which correspond to different baseline orientations into the sky-plane. This is a direct evidence for the shape of the $H\alpha$ emitting region being not spherical, but that it depends on the baseline orientation. According to Marlborough's (1997) measurements, ψ per is supposed to have an inclination angle of about 80 deg. Thus, its circumstellar disk could exhibit an elliptical elongation. This is also confirmed by our measurements. Unfortunately, due to a poor seeing during our observing run, we only have one measurement in the $H\beta$ line that impedes us to detect any departure from spherical symmetry.

In order to estimate the size of the $H\alpha$ and $H\beta$ emitting regions, we used an uniform disk to model the visibility measurement at the center of each emission line. To estimate properly the envelope sizes in $H\alpha$ and $H\beta$, we need to take into account also the effect of stellar continuum emission within each line. The visibility $V_{H\alpha}$ can

be written as:

$$V_{H\alpha} = \frac{V_{line}F_{line} - V_{cont}F_{cont}}{F_{line} - F_{cont}} \quad (3.1)$$

where $F_{H\alpha} = F_{line} - F_{cont}$

Following this equation, the corresponding $H\alpha$ emitting region has 4.04 mas as from the red curve and 3.21 mas from the green one, respectively when the sky-plane orientation are -20.92 and 18.38 degrees. The error bars, about 10 %, were estimated from the visibility fluctuations in the continuum. For the $H\beta$ emitting region, we have obtain a diameter of about 1.66 ± 0.1 mas.

The kinematics within the disk is related to the differential phase of fringes. With a small spectral resolution (smaller than the line width), we have only information on the global size of the emitting region at the studied wavelength. With a high spectral resolution, as the one available with VEGA (up to 30000), it is possible to study the kinematics within the line, since each spectral channel isolates one iso-velocity region with its own phase shift. Thus, following the phase shift as a function of wavelength, this is equivalent to follow the displacement of the photocenter of each iso-velocity curve, which reflects the velocity law within the disk, projected onto the line of sight. This technique, called ‘‘spectro-interferometry, is a very powerful tool to study in depth the kinematics in the Be star disks. Figure 2. shows the evolution of the phase of the visibility as a function of wavelength, called ‘‘differential phase:

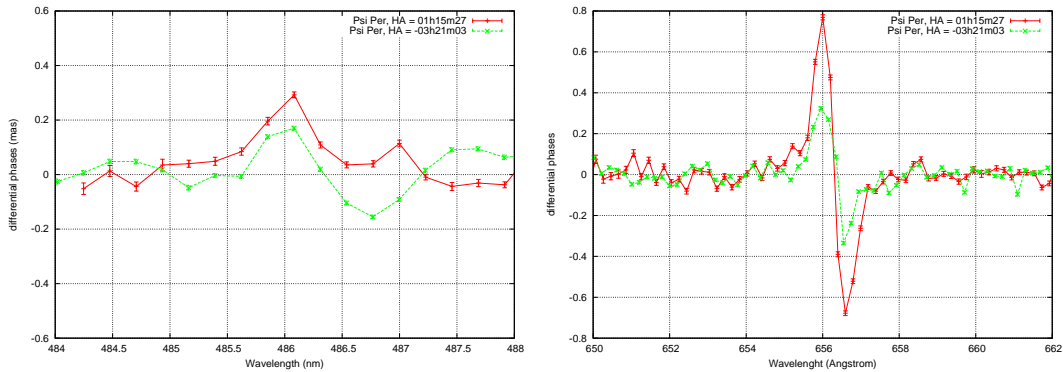


Fig. 2. Differential phase across the $H\beta$ (left) and $H\alpha$ (right) lines for ψ Per, at indicated HA for the S1S2 baseline.

The observed ‘‘S’’ shape is a clear signature indicating a rotating disk. The Keplerian rotation of the disk in α Arae was recently discovered by Meilland et al. (2007a), whereas in κ CMa such a disk rotation is not so clear, it could also be non-Keplerian (Meilland et al. 2007b). The differences between the amplitudes of the two ‘‘S’’, observed in Fig. 2, are due to the fact that the baseline orientations are different and thus, the projected photocenter displacement (or phase shift) are not the same (see Table 2). In practice, for a purely rotating disk the photocenter displacement is larger when the baseline is oriented along the major-axis of the disk.

4 Conclusions and perspectives

In this paper we present the study of the geometry of the ψ Per circumstellar environment, performed with the CHARA array and the VEGA focal instrument. Using a uniform disk model to interpret the interferometric observations, we have obtained two different diameters for the $H\alpha$ emitting region: 4.04 ± 0.4 mas and 3.21 ± 0.32 mas for baseline orientations respectively of -20.92 deg and 18.38 deg. These quantities carry evidence for the non-spherical nature of the circumstellar environment around this star. We have obtained only one diameter measurement of the $H\beta$ emitting region: 1.66 ± 0.1 mas for a baseline orientation of -20.92 deg, but cannot conclude on the spherical or non-spherical nature of the circumstellar environment at this wavelength. In a next step we shall try to fit our measurements using empirical kinematic models. The aim is to determine

the rotation law within the disk of ψ Per and the main parameters constraining the star + disk system, with the help of a global simulation of data with the SIMECA code (Stee & Araújo 1994; Stee & Bittar 2001).

References

- Arias, M.L., Zorec, J., Cidale, L. et al. 2006, A&A, 460, 821
Bjorkman, J. E., & Carciofi, A. C. 2004, A&A, 204, 6206
Dougherty, S. M., and Taylor A. R. 1992, Nature, 359, 808
Hanuschik, R. W., 1996, A&A, 308, 170
Kervella, P. & Domiciano de Souza, A. 2006, A&A, **453**, 1059
Marlborough, J. M., 1987, IAU Colloquium 92, ed. Sletterbak A., and Snow T. P., Cambridge, Cambridge University Press
Marlborough, J. M., Zijlstra, J.-W., Waters, L. B. F. M., 1997, ApJ, 321, 867
Poeckert, R., and Marlborough, J. M., 1978, ApJ, 220, 940
Quirrenbach, A., Bjorkman, K.S., Bjorkman, J.E., et al. 1997, ApJ, 479, 477
Stee, Ph., 1996, A&A, 311, 945
Stee, Ph., 2003, A&A, 403, 1023
Stee, Ph., Araújo, F. X., 1994, A&A, 292, 221
Stee, Ph., Bittar, J. 2001, SB, A &A, 367, 532
Struve, O., 1931, ApJ, 73, 94
Tycner, C., Jones, C. E., Sigut, T. A. A. et al., 2008, ApJ, 189, 461
Waters, L.B.F.M., 1986, A&A, 162, 121
Stee, P., Bittar, J.
Waters, L.B.F.M., Cot, J., Lamers, H.G.J.L.M., 1987, A&A, 185, 206
Waters, L.B.F.M., Marlborough, J. M., 1992, A&A, 253, L25
Zorec, J., Arias, M.L., Cidale, L. et al. 2007, A&A, 470, 239